

Large Scale Kernel Learning using Block Coordinate Descent

Stephen Tu * Rebecca Roelofs * Shivaram Venkataraman * Benjamin Recht *[†]

February 18, 2016

Abstract

We demonstrate that distributed block coordinate descent can quickly solve kernel regression and classification problems with millions of data points. Armed with this capability, we conduct a thorough comparison between the full kernel, the Nyström method, and random features on three large classification tasks from various domains. Our results suggest that the Nyström method generally achieves better statistical accuracy than random features, but can require significantly more iterations of optimization. Lastly, we derive new rates for block coordinate descent which support our experimental findings when specialized to kernel methods.

1 Introduction

Kernel methods are a powerful tool in machine learning, allowing one to discover non-linear structure by mapping data into a higher dimensional, possibly infinite, feature space. However, a known issue is that kernel methods do not scale favorably with dataset size. For instance, a naïve implementation of a kernel least squares solver requires $O(n^2)$ space and $O(n^3)$ time to store and invert the full kernel matrix. The prevailing belief is that when n reaches the millions, kernel methods are impractical.

This paper challenges the conventional wisdom by pushing kernel methods to the limit of what is practical on modern distributed compute platforms. We show that approximately solving a full kernel least squares problem with $n = 2 \times 10^6$ can be done in a matter of hours, and the resulting model achieves competitive performance in terms of classification errors. Mimicking the successes of the early 2000s, our algorithm is based on block coordinate descent and avoids full materialization of the kernel matrix [Joa99, FCL05].

Furthermore, in contrast to running multiple iterations in parallel and aggregating updates [AD11, NRRW11, ZWSL11, JST+14, LWR+15], we exploit distributed computation to parallelize *individual iterations* of block coordinate descent. We deliberately make this choice to alleviate communication overheads. Our resulting implementation inherits the linear convergence of block coordinate descent while efficiently scaling up to 1024 cores on 128 machines.

The capability to solve full kernel systems allows us to perform a direct head-to-head empirical comparison between popular kernel approximation techniques and the full kernel at an unprecedented scale. We conduct a thorough study of random features [RR07] and Nyström [WS01] approximations on three large datasets from speech, text, and image classification domains. Extending prior work comparing kernel approximations [YLM+12], our study is the first to work with multi-terabyte kernel matrices and to quantify computational versus statistical performance tradeoffs between the two methods at this scale. More specifically, we identify situations where the Nyström system requires significantly more iterations to converge than a random features system of the same size, but yields a better estimator when it does.

Finally, motivated by the empirical effectiveness of primal block coordinate descent methods in our own study and in related work that inspired our investigations [HAS+14], we derive a new rate of convergence for block coordinate descent on strongly convex smooth quadratic functions. Our analysis shows that block coordinate descent has a convergence rate that is no worse than gradient descent plus a small additive factor which is inversely proportional to the block size. Specializing this result to random features, Nyström, and kernel risk minimization problems corroborates our experimental findings regarding the iteration complexity of the three methods.

*Department of Electrical Engineering and Computer Science, UC Berkeley, Berkeley, CA.

[†]Department of Statistics, UC Berkeley, Berkeley, CA.

2 Background

This section concisely overviews the techniques used in this paper, and more importantly defines the specific optimization problems we solve. The theoretical underpinnings of kernel methods and their various approximations are well established in the literature; see e.g. [SS01] for a thorough treatment.

Notation. For a vector x , we let $\|x\|$ denote the Euclidean norm. For a matrix X , we let $\|X\|$ denote the operator norm, $\|X\|_F$ the Frobenius norm, and $\sigma_1(X) \geq \sigma_2(X) \geq \dots \geq \sigma_r(X) > 0$ denote the singular values of X in decreasing order, where $r = \text{rank}(X)$. If X is symmetric, let $\lambda_{\max}(X), \lambda_{\min}(X)$ denote the maximum and minimum eigenvalues of X , respectively. For two conforming matrices A and B , $\langle A, B \rangle := \text{Tr}(A^\top B)$.

Finally, given a matrix $X \in \mathbb{R}^{n_1 \times n_2}$ and two index sets $I \in 2^{[n_1]}, J \in 2^{[n_2]}$, we let $X(I, J) \in \mathbb{R}^{|I| \times |J|}$ denote the submatrix of X which selects out the rows in I and the columns in J .

2.1 Kernel methods and approximations

Let \mathcal{H} be a reproducing kernel Hilbert space (RKHS) of functions $f : \mathcal{X} \rightarrow \mathbb{R}$, with associated Mercer kernel $\kappa : \mathcal{X} \times \mathcal{X} \rightarrow \mathbb{R}$. We typically associate \mathcal{X} with \mathbb{R}^d .

Given a set of data points $\{(x_i, y_i)\}_{i=1}^n$ with $x_i \in \mathcal{X}$ and $y_i \in \{1, 2, \dots, k\}$, we use the standard one-versus-all (OVA) approach [RK04] to turn a multiclass classification problem into k binary classification problems of the form

$$\min_{f_j \in \mathcal{H}} \frac{1}{n} \sum_{i=1}^n \ell(f_j(x_i), y_{ij}) + \lambda \|f_j\|_{\mathcal{H}}^2, \quad j = 1, \dots, k, \quad (1)$$

where y_{ij} is 1 if $y_i = j$ and -1 otherwise. While in general ℓ can be any convex loss function, we focus on the square loss $\ell(a, b) = (a - b)^2$ to make the algorithmic and systems comparisons more transparent. While other loss functions like softmax, logistic, or hinge losses are frequently used for classification, regularized least squares classification performs as well in most scenarios [Rif02, RR07, AKK⁺13]. Furthermore, a least squares solver can be bootstrapped into a minimizer for general loss functions with little additional cost using a splitting method such as ADMM [BPC⁺11, ZKR14].

Owing to the representer theorem, minimization over \mathcal{H} in (1) is equivalent to minimization over \mathcal{H}_n , where $\mathcal{H}_n := \text{span}\{\kappa(x_i, \cdot) : i = 1, \dots, n\}$. Therefore, defining $K \in \mathbb{R}^{n \times n}$ as $K_{ij} := \kappa(x_i, x_j)$, we can write (1) as

$$\min_{\alpha \in \mathbb{R}^{n \times k}} \frac{1}{n} \|K\alpha - Y\|_F^2 + \lambda \langle \alpha, K\alpha \rangle, \quad (2)$$

where $Y \in \mathbb{R}^{n \times k}$ is a label matrix with $Y_{ij} = 1$ if $y_i = j$ and -1 otherwise. The normal equation of (2) is

$$K(K + n\lambda I_n)\alpha = KY.$$

Solutions of (2) take on the form $\alpha_* = (K + n\lambda I_n)^{-1}Y + Q$, with $Q \in \mathbb{R}^{n \times k}$ satisfying $KQ = 0_{n \times k}$. The resulting f is $f(x) = (\kappa(x, x_1), \dots, \kappa(x, x_n))^\top \alpha_* \in \mathbb{R}^{1 \times k}$.

Nyström method. Let $I \in 2^{[n]}$ denote an index set of size p , and let $K_I := K([n], I)$, $K_{II} := K(I, I)$. One common variant of the Nyström method [WS01, DM05, GM13, BJ05] is to use the matrix $\widehat{K} := K_I K_{II}^\dagger K_I^\top$ as a low rank approximation to K (2). An alternative approach is to first replace the minimization over \mathcal{H} in (1) with \mathcal{H}_I , where $\mathcal{H}_I := \text{span}\{\kappa(x_i, \cdot) : i \in I\}$. We then arrive at the optimization problem

$$\min_{\alpha \in \mathbb{R}^{p \times k}} \frac{1}{n} \|K_I \alpha - Y\|_F^2 + \lambda \langle \alpha, K_{II} \alpha \rangle, \quad (3)$$

with $f(x) = (\kappa(x, x_{I(1)}), \dots, \kappa(x, x_{I(p)}))^\top \alpha_* \in \mathbb{R}^{1 \times k}$. The normal equation for (3) is

$$(K_I^\top K_I + n\lambda K_{II})\alpha = K_I^\top Y,$$

and hence solutions take on the form $\alpha_* = (K_I^\top K_I + n\lambda K_{II})^\dagger K_I^\top Y + Q$, with $Q \in \mathbb{R}^{p \times k}$ satisfying $K_I Q = 0_{p \times k}$. For numerical stability reasons, one might pick a small $\gamma > 0$ and solve instead

$$(K_I^\top K_I + n\lambda K_{II} + n\lambda\gamma I_p)\alpha = K_I^\top Y.$$

This extra regularization is justified statistically by [Bac13, EM15].

Random features. Random feature based methods [RR07] use an element-wise approximation of K . Suppose that (Ω, ρ) is a measure space and $\varphi : \mathcal{X} \times \Omega \rightarrow \mathbb{R}$ is a measurable function such that for all $x, y \in \mathcal{X}$, $\mathbb{E}_{\omega \sim \rho} \varphi(x, \omega)\varphi(y, \omega) = \kappa(x, y)$. Random feature approximations works by drawing $\omega_1, \dots, \omega_p \stackrel{\text{iid}}{\sim} \rho$ and defining the map $z : \mathcal{X} \rightarrow \mathbb{R}^p$ as

$$z(x) := \frac{1}{\sqrt{p}}(\varphi(x, \omega_1), \dots, \varphi(x, \omega_p)).$$

The optimization of f in (1) is then restricted to the space $\mathcal{H}_\rho := \text{span}\{z(x_i)^\top z(\cdot) : i = 1, \dots, n\}$. Define $Z \in \mathbb{R}^{n \times p}$ as $Z := (z(x_1), \dots, z(x_n))^\top$. Applying the same argument as before followed by an appropriate change of variables, we can solve the program in primal form

$$\min_{w \in \mathbb{R}^{p \times k}} \frac{1}{n} \|Zw - Y\|_F^2 + \lambda \|w\|_F^2. \quad (4)$$

The normal equation for (4) is

$$(Z^\top Z + n\lambda I_p)w = Z^\top Y,$$

and hence $w_* = (Z^\top Z + n\lambda I_p)^{-1} Z^\top Y$ and $f(x) = z(x)^\top w_* \in \mathbb{R}^{1 \times k}$.

Note that when $\mathcal{X} = \mathbb{R}^d$ and $\kappa(x, y) = \kappa(\|x - y\|)$ is translation invariant, Bochner's theorem states that the (scaled) Fourier transform of $\kappa(\cdot)$ will be a valid probability measure on \mathbb{R}^d . The map φ can then be constructed as $\varphi(x, (\omega, b)) = \sqrt{2} \cos(x^\top \omega + b)$, where ω is drawn from the Fourier transform of $\kappa(\cdot)$ and $b \sim \text{Unif}([0, 2\pi])$.

2.2 Related work

An empirical comparison on Nyström versus random features was done by Yang et al. [YLM⁺12]. This study demonstrated that the Nyström method outperformed random features on every dataset in their experiments. Our experimental efforts differ from this seminal work in several ways. First, we quantify time versus statistical performance tradeoffs, instead of studying only the empirical risk minimizer. Second, we describe a scalable algorithm which allows us to compare performance with the full kernel. Finally, our datasets are significantly larger, and we also sweep across a much wider range of number of random features.

On the algorithms side, the inspiration for this work was by Huang et al. [HAS⁺14], who devised a similar block coordinate descent algorithm for solving random feature systems. In this work, we extend the block coordinate algorithm to both the full kernel and Nyström systems. This enables us to train the full kernel on the entire TIMIT dataset, achieving a lower test error than the random feature approximations.

3 Algorithms

The optimal solutions written in Section 2.1 require solving large linear systems where the data cannot be assumed to fit entirely in memory. This necessitates a different algorithm than the least squares solvers implemented in standard library routines. Fortunately, for the statistical problems we are interested in, obtaining a high accuracy solution is not as important. Hence, we propose to use block coordinate descent [BT89], which admits a natural distributed implementation, and, in our experience, converges to a reasonable accuracy after only a few passes through the data.

Coordinate methods in machine learning. Coordinate methods in machine learning date back to the late 90s with SVMLight [Joa99] and SMO [Pla98]. More recently, many researchers [Yan13, RT13, JST⁺14, MSJ⁺15] have proposed using distributed computation to run multiple iterations of coordinate descent in parallel. As noted previously, we take a different approach and use distributed computing to accelerate within an iteration. This is similar to [HCL⁺08, YHCL10], both who describe block coordinate algorithms for solving SVMs. However, using the square loss instead of hinge loss simplifies our analysis and implementation.

3.1 Block coordinate descent

We first describe block coordinate descent generically and then specialize it for the least squares loss. Let $f : \mathbb{R}^d \rightarrow \mathbb{R}$ be a twice differentiable strongly convex, smooth function, and let $b \in \{1, \dots, d\}$ denote a block size. Let $I \in 2^{[d]}$ be an index set such that $|I| = b$, and let $P_I : \mathbb{R}^d \rightarrow \mathbb{R}^d$ be the projection operator which zeros out all coordinates $j \notin I$, leaving coordinates $i \in I$ intact. Block coordinate descent works by iterating the mapping

$$w^{\tau+1} \leftarrow w^\tau - \Gamma_\tau \cdot P_{I^c} \nabla f(w^\tau),$$

where I_τ is drawn at random by some sampling strategy (typically uniform), and $\Gamma_\tau \in \mathbb{R}^{d \times d}$ is either fixed, or chosen by direct line search. We choose the latter, in which case we write

$$w^{\tau+1} \leftarrow \operatorname{argmin}_{w \in \mathbb{R}^d} f(P_{I_\tau^c} w^\tau + P_{I_\tau} w). \quad (5)$$

In the case where f is least squares, the update (5) is equivalent to block Gauss-Seidel on the normal equations. For instance, for (4), the update (5) reduces to solving the $b \times b$ equation

$$w_{I_\tau}^{\tau+1} \leftarrow (Z_{I_\tau}^\top Z_{I_\tau} + n\lambda I_b)^{-1} Z_{I_\tau}^\top Y, \quad (6)$$

where $Z_{I_\tau} := Z([n], I_\tau)$. The w_{I_τ} notation means we set only the coordinates in I_τ equal to the RHS, and the coordinates not in I_τ remain the same from the previous iteration.

Distributed execution. We solve block coordinate descent in parallel by distributing the computation of $Z_{I_\tau}^\top Z_{I_\tau}$ and $Z_{I_\tau}^\top Y$. To do this, we partition the rows of Z_{I_τ} , Y across all the machines in a cluster and compute the sum of outer products from each machine. The result of this distributed operation is a $b \times b$ matrix and we pick b such that the solve for $w_{I_\tau}^{\tau+1}$ can be computed quickly using existing lapack solvers on a single machine.

Choosing an appropriate value of b is important as it affects both the statistical accuracy and run-time performance. Using a larger value for b leads to improved convergence and is also helpful for using BLAS-3 primitives in single machine operations. However, a very large value for b increases the serial execution time and the communication costs. In practice, we see that setting b in the range 2,000 to 8,000 offers a good trade-off.

Block generation primitives. As mentioned previously, our algorithms only require a procedure that materializes a column block at a time. We denote this primitive by `KERNELBLOCK`(X, I), where X represents the data matrix and I is a list of column indices. The output of `KERNELBLOCK` is $K([n], I)$. After a column block is used in a block coordinate descent update of the model, it can be immediately discarded. We also use distributed computation to parallelize the generation of a block K_{I_τ} of the kernel matrix. We also define a similar primitive, `RANDOMFEATURESBLOCK`(X, I), which returns $Z([n], I)$ for random feature systems.

3.2 Algorithm descriptions

Full kernel block coordinate descent. Our full kernel solver is described in Algorithm 1. Algorithm 1 is actually Gauss-Seidel on the linear system $(K + n\lambda I_n)\alpha = Y$, but as we will discuss in Section 4.3, this is equivalent to block coordinate descent on a modified objective function (which is strongly convex, even when K is rank deficient). See [HNR15] for a similar discussion in the context of ridge regression.

ALGORITHM	COMPUTATION	COMMUNICATION
FULL KERNEL	$(\frac{nbk}{M} + b^3) \times \frac{n}{b}$	$b^2 \times \frac{n}{b}$
NYSTRÖM/RF.	$(\frac{nb^2}{M} + \frac{nbk}{M} + b^3) \times \frac{p}{b}$	$\log(M)b^2 \times \frac{p}{b}$

Table 1: Computation and communication costs for one epoch of distributed block coordinate descent. The number of examples is n , the number of features is p , the block size is b , the number of classes is k , and the number of machines is M . Each cost is presented as (cost for one block) \times (number of blocks).

Algorithm 1 Full kernel block coordinate descent

Input: data $X \in \mathcal{X}^n$, $Y \in \{\pm 1\}^{n \times k}$,
number of epochs n_e ,
block size $b \in \{1, \dots, n\}$,
regularizer $\lambda > 0$.

Assume: n/b is an integer.
 $\pi \leftarrow$ random permutation of $\{1, \dots, n\}$.
 $\mathcal{I}_1, \dots, \mathcal{I}_{\frac{n}{b}} \leftarrow$ partition π into $\frac{n}{b}$ pieces.
 $\alpha \leftarrow 0_{n \times k}$.

for $\ell = 1$ **to** n_e **do**
 $\pi \leftarrow$ random permutation of $\{1, \dots, \frac{n}{b}\}$.
for $i = 1$ **to** $\frac{n}{b}$ **do**
 $K_b \leftarrow \text{KERNELBLOCK}(X, \mathcal{I}_{\pi_i})$.
 $Y_b \leftarrow Y(\mathcal{I}_{\pi_i}, [k])$.
 $R \leftarrow 0_{b \times k}$.
for $j \in \{1, \dots, \frac{n}{b}\} \setminus \{\pi_i\}$ **do**
 $R \leftarrow R + K_b(\mathcal{I}_{\pi_i}, [b])^\top \alpha(\mathcal{I}_{\pi_i}, [b])$.
end for
Solve $(K_b(\mathcal{I}_{\pi_i}, [b]) + \lambda I_b)\alpha_b = Y_b - R$.
 $\alpha(\mathcal{I}_{\pi_i}, [k]) \leftarrow \alpha_b$.
end for
end for

Nyström block coordinate descent. Unlike the full kernel case, our Nyström implementation operates directly on the normal equations. A notable point of our algorithm is that it does *not* require computation of the pseudo-inverse K_{II}^\dagger . When the number of Nyström features is large, calculating the pseudo-inverse K_{II}^\dagger is expensive in terms of computation and communication. By making K_{II} a part of the block coordinate descent update we are able to handle large number of Nyström features while only needing a block of features at a time.

We denote $\text{SELECTOR}(n, I)$ as the function which returns an $\{0, 1\}^{n \times |I|}$ matrix S such that $S_{I(j)j} = 1$ and zero otherwise, for $j = 1, \dots, |I|$; this is simply the column selector matrix associated with the indices in I . Using the above notation, the Nyström algorithm is described in Algorithm 2.

Random features block coordinate descent. Our random features solver is the same as Algorithm 2 from [HAS⁺14]. We include it in Algorithm 3 for completeness.

Computation and communication overheads. Table 1 summarizes the computation and communication costs of the algorithms presented below. The computation costs in the full kernel are associated with computing the residual R and solving a $b \times b$ linear system. For the Nyström method (and random features), the computation costs include computing $K_j^\top K_I$, $K_j^\top Y$ in parallel and a similar local solve. Computing the gram matrix however requires adding

Algorithm 2 Nyström block coordinate descent

Input: data $X \in \mathcal{X}^n$, $Y \in \{\pm 1\}^{n \times k}$,
number of epochs n_e ,
number of Nyström features $p \in \{1, \dots, n\}$,
block size $b \in \{1, \dots, p\}$.
regularizers $\lambda > 0, \gamma \geq 0$.

Assume: p/b is an integer.

$\mathcal{J} \leftarrow p$ without replacement draws from $\{1, \dots, n\}$.
 $\mathcal{I}_1, \dots, \mathcal{I}_{\frac{p}{b}} \leftarrow$ partition \mathcal{J} into $\frac{p}{b}$ pieces.
 $\alpha \leftarrow 0_{p \times k}$, $R \leftarrow 0_{n \times k}$.

for $\ell = 1$ **to** n_e **do**
 $\pi \leftarrow$ random permutation of $\{1, \dots, \frac{n}{b}\}$.
 for $i = 1$ **to** $\frac{p}{b}$ **do**
 $B \leftarrow \{(\pi_i - 1)b + 1, \dots, \pi_i b\}$.
 $\alpha_b \leftarrow \alpha(B, [k])$.
 $S_b \leftarrow \text{SELECTOR}(n, \mathcal{I}_{\pi_i})$.
 $K_b \leftarrow \text{KERNELBLOCK}(X, \mathcal{I}_{\pi_i})$.
 $R \leftarrow R - (K_b + n\lambda S_b)\alpha_b$.
 $K_{bb} \leftarrow K_b(\mathcal{I}_{\pi_i}, [b])$.
 Solve $(K_b^\top K_b + n\lambda K_{bb} + n\lambda\gamma I_b)\alpha'_b = K_b^\top(Y - R)$.
 $R \leftarrow R + (K_b + n\lambda S_b)\alpha'_b$.
 $\alpha(B, [k]) \leftarrow \alpha'_b$.
 end for
end for

M matrices of size $b \times b$. Using a tree-based aggregation, this results in $O(\log(M)b^2)$ bytes being transferred. We study how these costs matter in practice in Section 5.

Computing the regularization path. Algorithms 1, 2, and 3 are all described for a single input λ . In practice, for model selection, one often computes an estimator for multiple values of λ . The naïve way of doing this is to run the algorithm again for each value of λ . However, a faster approach, which we use in our experiments, is to maintain separate models α_λ and separate residuals R_λ for each value of λ , and reuse the computation of the block matrices K_b for full kernel, $K_b^\top K_b$ for Nyström, and $Z_b^\top Z_b$ for random features. We can do this because the block matrices do not depend on the value of λ . As we show in Section 5, in each iteration of our algorithms, a large fraction of time is spent in computing these block matrices; thus this optimization allows us compute solutions for multiple λ values for essentially the price of a single solution.

We would like to note that in the case of Nyström approximations, [RCR15] provides an algorithm for computing the regularization path along p , the number of Nyström samples, by using rank-one Cholesky updates. We leave it as future work to see if a similar technique can be applied to our Nyström block coordinate algorithm.

4 Optimization and statistical rates

In this section we present our theoretical results which characterize optimization error for kernel methods. All proofs are deferred to the appendix.

Known convergence rates. We start by stating the existing rates for block coordinate descent. To do this, we define a restricted Lipschitz constant as follows. For any $Q(\cdot)$ such that $Q(x) \succeq 0$ for all x , define

$$L_{\max, b}(Q(\cdot)) := \sup_{x \in \mathbb{R}^d} \max_{|I|=b} \lambda_{\max}(P_I Q(x) P_I).$$

Algorithm 3 Random features block coordinate descent

Input: data $X \in \mathcal{X}^n$, $Y \in \{\pm 1\}^{n \times k}$.
number of epochs n_e ,
number of random features $p \geq 1$,
block size $b \in \{1, \dots, p\}$.
regularizers $\lambda > 0$.

Assume: p/b is an integer.

$\pi \leftarrow$ random permutation of $\{1, \dots, p\}$.

$\mathcal{I}_1, \dots, \mathcal{I}_{\frac{p}{b}} \leftarrow$ partition π into $\frac{p}{b}$ pieces.

$w \leftarrow 0_{p \times k}$.

$R \leftarrow 0_{n \times k}$

for $\ell = 1$ **to** n_e **do**

$\pi \leftarrow$ random permutation of $\{1, \dots, \frac{p}{b}\}$.

for $i = 1$ **to** $\frac{p}{b}$ **do**

$I \leftarrow \mathcal{I}_{\pi_i}$.

$Z_b \leftarrow \text{RANDOMFEATURESBLOCK}(X, I)$.

$R \leftarrow R - Z_b w(I, [k])$.

Solve $(Z_b^\top Z_b + n\lambda I_b)w_b = Z_b^\top(Y - R)$.

$R \leftarrow R + Z_b w_b$.

$w(I, [k]) \leftarrow w_b$.

end for

end for

Standard analysis of block coordinate descent (see e.g. Theorem 1 of [Wri15]) states that to reach accuracy $\mathbb{E}f(w^\tau) - f_* \leq \epsilon$, one requires at most

$$\tau \leq O\left(\frac{dL_{\max,b}}{bm} \log \epsilon^{-1}\right) \quad (7)$$

iterations, where $L_{\max,b} := L_{\max,b}(\nabla^2 f(\cdot))$.

While $L_{\max,b} \leq \sup_{x \in \mathbb{R}^d} \lambda_{\max}(\nabla^2 f(x))$ always, it is easy to construct cases where the inequality is tight¹. In this case, the upper bound (7) dictates that d/b more iterations of block coordinate descent are needed to reach the same error tolerance as the incremental gradient method.

4.1 Improved rate for quadratic functions

In our experience, the case where block coordinate descent needs d/b times more iterations does not occur in practice. To address this, we improve the analysis in the case of strongly convex and smooth quadratic functions to depend only on a quantity which behaves like the *expected* value $\mathbb{E}_I \lambda_{\max}(P_I \nabla^2 f P_I)$ where I is drawn uniformly.

Theorem 4.1. *Let $f : \mathbb{R}^d \rightarrow \mathbb{R}$ be a quadratic function with Hessian $\nabla^2 f \in \mathbb{R}^{d \times d}$, and assume for some $L \geq m > 0$,*

$$m \leq \lambda_{\min}(\nabla^2 f), \quad \lambda_{\max}(\nabla^2 f) \leq L.$$

Let w^τ denote the τ -th iterate of block coordinate descent with the index set I_τ consisting of $b \in \{1, \dots, d\}$ indices drawn uniformly at random without replacement from $\{1, \dots, d\}$. The iterate w^τ satisfies

$$\mathbb{E}f(w^\tau) - f_* \leq \left(1 - \frac{m}{2L_{\text{eff}}}\right)^\tau (f(w^0) - f_*),$$

where

$$L_{\text{eff}} := e^2 L + \frac{d \log(2d^2/b)}{b} \|\text{diag}(\nabla^2 f)\|_\infty.$$

¹Take, for instance, any block diagonal matrix where the blocks are of size b .

$\sigma_\ell(K)$ EXPONENTIAL DECAY			$\sigma_\ell(K)$ POLYNOMIAL DECAY	
METHOD	ITERATIONS	BLOCK SIZE	ITERATIONS	BLOCK SIZE
FULL	$\tilde{O}(n)$	$\Omega(\log^2 n)$	$\tilde{O}(n^{\frac{2\beta}{2\beta+1}})$	$\Omega(n^{1/(2\beta+1)} \log n)$
NYSTRÖM	$\tilde{O}(np/\gamma)$	$\Omega((1+\gamma) \log n)$	$\tilde{O}(pn^{\frac{2\beta}{2\beta+1}}/\gamma)$	$\Omega((1+\gamma) \log n)$
R.F.	$\tilde{O}(n)$	$\Omega(\log n)$	$\tilde{O}(n^{\frac{2\beta}{2\beta+1}})$	$\Omega(\log n)$

Table 2: Iteration complexity and block size requirements of solving a full kernel system with block coordinate descent versus Nyström and random feature approximations. For both Nyström/RF, we assume that $p \gtrsim \log n$, and for Nyström we assume the regularized objective with $\gamma > 0$ (see Section 2.1). Finally, for both Nyström/RF, the bounds hold w.h.p. over the feature sampling.

Theorem 4.1 states that in order to reach an ϵ -sub-optimal solution for f , the number of iterations required is at most

$$O\left(\left(\frac{L}{m} + \frac{1}{b} \frac{d \log d}{m} \|\text{diag}(\nabla^2 f)\|_\infty\right) \log \epsilon^{-1}\right). \quad (8)$$

That is, block coordinate descent pays the rate of gradient descent plus $1/b$ times the rate of standard ($b = 1$) coordinate descent (ignoring log factors). To see that this can be much better than the standard rate (7), suppose that $d = p^2$ for some $p \geq 1$, and consider any quadratic with Hessian

$$\nabla^2 f = \lambda I_d + \text{diag}(\mathbf{1}_{\sqrt{d}} \mathbf{1}_{\sqrt{d}}^\top, \dots, \mathbf{1}_{\sqrt{d}} \mathbf{1}_{\sqrt{d}}^\top) \in \mathbb{R}^{d \times d},$$

where $\mathbf{1}_\ell \in \mathbb{R}^\ell$ is the all ones vector. If we set $b = \sqrt{d}$, the rate from (7) requires $\tilde{O}(d/\lambda)$ iterations to reach tolerance ϵ , whereas the rate from Theorem 4.1 requires only $\tilde{O}(\sqrt{d}/\lambda)$ to reach the same tolerance.

Equation (8) suggests setting b such that the second term matches L/m order wise. That is, as long as $b \gtrsim d \log d \|\text{diag}(\nabla^2 f)\|_\infty / L$, we have that at most $\tilde{O}(L/m)$ iterations are necessary². In the sequel, we will assume this setting of b .

We highlight the main ideas behind the proof of Theorem 4.1. The proof proceeds in two steps. First, we establish a structural result which states that, given a large set \mathcal{G} of indices where the restricted Lipschitz constant of the Hessian is well controlled, the overall dependence on Lipschitz constant is not much worse than the maximum Lipschitz constant restricted to \mathcal{G} . Second, we use a probabilistic argument to show that such a set \mathcal{G} does indeed exist. The first result is based on a modification of the standard coordinate descent proof, whereas the second result is based on a matrix Chernoff argument.

4.2 Rates for kernel optimization

We now specialize Theorem 4.1 to the optimization problems described in Section 2.1. We assume the asymptotic setting [Bra06] where $\sigma_\ell(K) = n \cdot \mu_\ell$ for (a) exponential decay $\mu_\ell = e^{-\rho\ell}$ with $\rho > 0$ and (b) polynomial decay $\mu_\ell = \ell^{-2\beta}$ with $\beta > 1/2$. We also set λ to be the minimax optimal rate [DFH15] for the settings of (a) and (b): for exponential decay $\lambda = \log n/n$ and for polynomial decay $\lambda = n^{-\frac{2\beta}{2\beta+1}}$. Finally, we assume that $\sup_{x_1, x_2 \in \mathcal{X}} \kappa(x_1, x_2) \leq O(1)$.

Table 2 quantifies the iteration complexity of solving the full kernel system versus the Nyström and random features approximation. Our worst case analysis shows that the Nyström system requires roughly p times more iterations to solve than random features. This difference is due to the inability to reduce the Nyström normal equation from quadratic in K to linear in K , as is done in the full kernel normal equation. Indeed, the Nyström method is less well conditioned in practice, and we observe similar phenomena in our experiments below. The derivation of the bounds in Table 2 is deferred to Appendix B.

² We use the notation $x \gtrsim y$ to mean there exists an absolute constant $C > 0$ such that $x \geq Cy$, and $\tilde{O}(\cdot)$ to suppress dependence on poly-logarithmic terms.

DATASET	n	d	k	SIZE (TB)
TIMIT	2,251,569	440	147	40.56
YELP	1,255,412	65,282,968	5	12.61
CIFAR-10	500,000	4096	10	2.00

Table 3: Datasets used for evaluation. Here n , d , k refer to the number of training examples, features and classes respectively. Size represents the size of the full kernel matrix in terabytes.

4.3 Primal versus dual coordinate methods

Duality gives us a choice as to whether to solve the primal or dual problem; strong duality asserts that both solutions are equivalent. We can use this freedom to our advantage, picking the formulation which yields the most numerically stable system. For instance, in the full kernel solver we chose to work with the system $(K + n\lambda I_n)\alpha = Y$ instead of $K(K + n\lambda I_n)\alpha = KY$. The former is actually the dual system, and the latter is the primal. Here, the primal system has a condition number which is roughly the square of the dual.

On the other hand, for both Nyström and random features, our system works on the primal formulation. This is intuitively desirable since $p \ll n$ and hence the primal system is much smaller. However, some authors including [SSZ13] advocate for the dual formulation even when $p \ll n$. We claim that, at least in the case of random Fourier features, their argument does not apply.

To do this, we consider the random features program with $b = k = 1$, which fits the framework of [SSZ13] the closest. By the primal-dual correspondence $w = \frac{1}{n\lambda} Z^T \alpha$, the dual program is

$$\max_{\alpha \in \mathbb{R}^n} \frac{1}{n} Y^T \alpha - \frac{1}{n} \|\alpha\|^2 - \frac{1}{\lambda n^2} \alpha^T Z Z^T \alpha.$$

Theorem 5 from [SSZ13] states that $O((n + L_{\max,1}(ZZ^T)/\lambda) \log \epsilon^{-1})$ iterations of dual coordinate ascent are sufficient to reach an ϵ -sub-optimal primal solution. On the other hand, Equation (7) yields that at most $O((pL_{\max,1}(Z^T Z)/n\lambda) \log \epsilon^{-1})$ iterations of primal coordinate descent are sufficient to reach the same accuracy.

For random Fourier features, both $L_{\max,1}(ZZ^T)$ and $L_{\max,1}(Z^T Z)$ can be easily upper bounded, since $|\langle z(x_i), z(x_i) \rangle| \leq \frac{2}{p} \sum_{k=1}^p |\cos(x_i^T w_k + b_k)| \leq 2$ and also $\|\text{diag}(Z^T Z)\|_\infty = \max_{1 \leq k \leq p} \frac{2}{p} \sum_{i=1}^n \cos^2(w_k^T x_i + b_k) \leq \frac{2n}{p}$. Therefore, the dual rate is $\tilde{O}(n + 1/\lambda)$ and the primal rate is $\tilde{O}(1/\lambda)$. That is, for random Fourier features, the primal rate upper bound beats the dual rate upper bound.

5 Experiments

This section describes our experimental evaluation. We implement our algorithms in Scala on top of Apache Spark [ZCD⁺12]. Our experiments are run on Amazon EC2, with a cluster of 128 r3.2xlarge machines, each of which has 4 physical cores and 62 GB of RAM.

We measure classification accuracy for three large datasets spanning speech (TIMIT), text (Yelp), and vision (CIFAR-10). The size of these datasets are summarized in Table 3. For all our experiments, we set the block size to $b = 6144$. We shuffle the raw data at the beginning of the algorithm, and select blocks in a random order for block coordinate descent. For the Nyström method, we uniformly sample p columns without replacement from the full kernel matrix.

5.1 TIMIT

We evaluate a phone classification task on the TIMIT dataset³, which consists of spoken audio from 462 speakers. We use the same preprocessing pipeline as [HAS⁺14], resulting in 2.25×10^6 training examples and 10^5 test examples.

³<https://catalog.ldc.upenn.edu/LDC93S1>

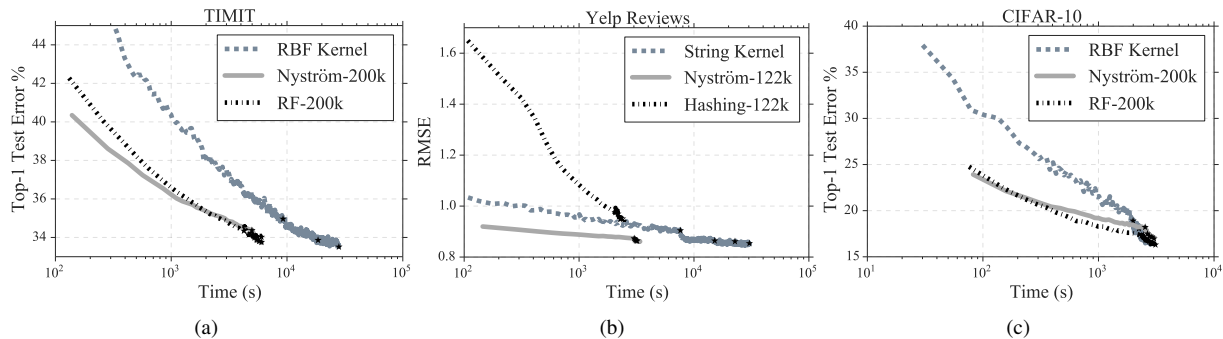


Figure 1: Comparison of classification error using different methods on the TIMIT, Yelp, and CIFAR-10 datasets. We measure the test error after every block of the algorithm; black stars denote the end of an epoch.

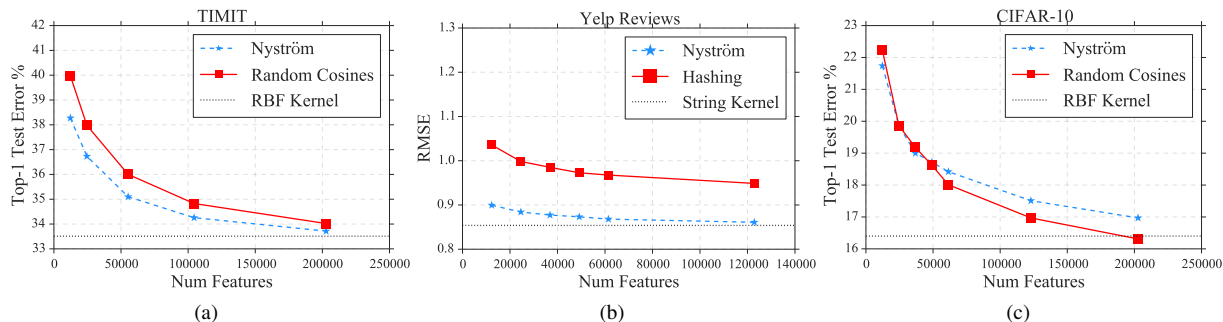


Figure 2: Classification error as we increase the number of features for Nyström, Random Features on the TIMIT, Yelp, and CIFAR-10.

The preprocessing pipeline produces a dense vector with 440 features and we use a shuffled version of this as the input to our kernel methods. We apply a Gaussian (RBF) kernel for the Nyström and exact methods and use random cosines [RR07] for the random feature method. Figure 1(a) shows the top-1 test error for each technique. From the figure, we can see that while the exact method takes the longest to complete a full epoch (around 2.5 hours), it achieves the lowest top-1 test-error (33.51%) among all methods after 3 epochs. Furthermore, unlike the exact method, the data for the Nyström and random features with $p = 200,000$ can be cached in memory; as a result, the approximate methods run much faster after the first epoch compared to the exact method.

We also compare Nyström and random features by varying p in Figure 2(a) and find that for $p \geq 100,000$ both methods approach the test error of the full kernel within 1%.

5.2 Yelp Reviews

We next evaluate a text classification task where the goal is to predict a rating from one to five stars from the text of a review. The data comes from Yelp’s academic dataset⁴, which consists of 1.5×10^6 customer reviews. We set aside 20% of the reviews for test, and train on the remaining 80%. For preprocessing, we use `nlTK`⁵ for tokenizing and stemming documents. We then remove English stop words and create 3-grams, resulting in a sparse vector with dimension 6.52×10^7 . For the exact and Nyström experiments, we apply a linear kernel, which when combined with the 3-grams can be viewed as an instance of a string kernel [SRR07]. For random features, we apply a hash kernel [WDL⁺09] using MurmurHash3 as our hash function. Since we are predicting ratings for a review, we measure accuracy by using the root mean square error (RMSE) of the predicted rating as compared to the actual rating. Figure 1(b) shows how

⁴https://www.yelp.com/academic_dataset

⁵<http://www.nltk.org/>

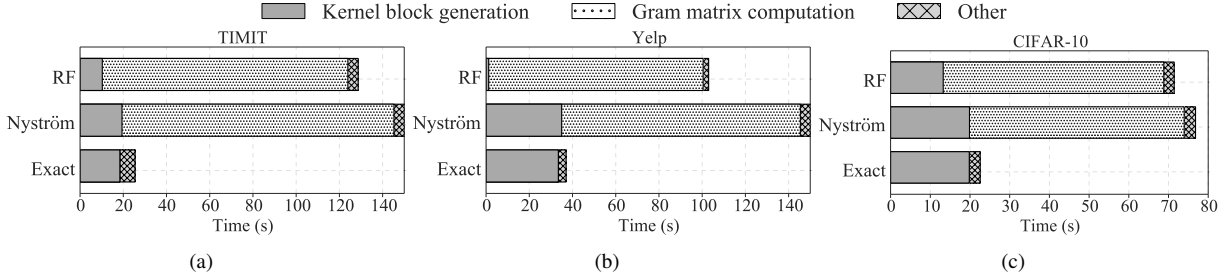


Figure 3: Breakdown of time to compute a *single* block in the first epoch on the TIMIT, CIFAR-10, and Yelp datasets.

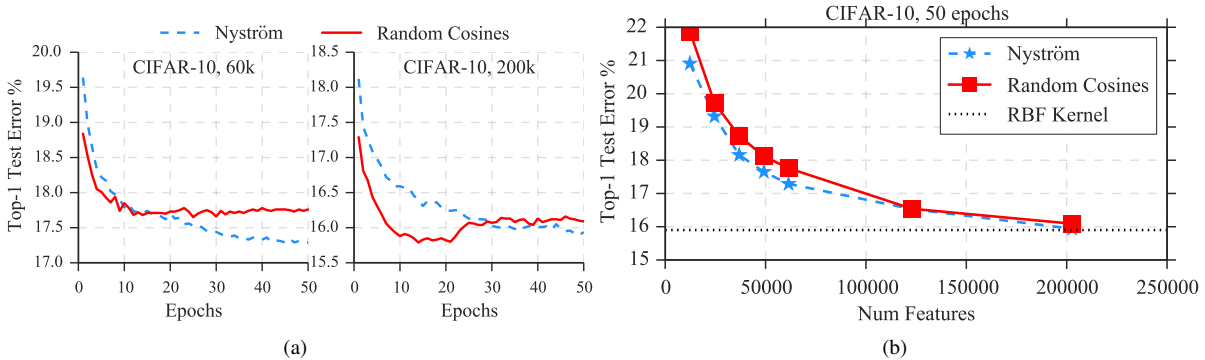


Figure 4: Convergence rate, Top-1 test error for CIFAR-10 across 50 epochs for Nyström and random features.

various kernel methods perform with respect to wall clock time. From the figure, we can see that the string kernel performs much better than the hash-based random features for this classification task. We also see that the Nyström method achieves almost the same RMSE (0.861) as the full kernel (0.854) when using 122,000 features. Finally, Figure 2(b) shows that the improved accuracy from using the string kernel over hashing holds as we vary the number of features (p) for the Nyström and random feature methods.

5.3 CIFAR-10

Our last task involves image classification for the CIFAR-10 dataset ⁶. We perform the same data augmentation as described in `cuda-convnet2` ⁷, which results in 500,000 train images. For preprocessing, we use a pipeline similar to [CN12], replacing the k -means step with random image patches. Using 512 random image patches, we get 4096 features per image and fitting a linear model with these features gives us 25.7% test error. For our kernel methods, we start with these 4096 features as the input and we use the RBF kernel for the exact and Nyström method and random cosines for the random features method.

From Figure 1(c), we see that on CIFAR-10 the full kernel takes around the same time as Nyström and random features. This is because we have fewer examples ($n = 500,000$) and this leads to fewer blocks that need to be solved per-epoch. We are also able to cache the entire kernel matrix in memory ($\sim 2TB$) in this case and this provides a speedup after the first epoch.

Furthermore, as shown in Figure 2(c), we see that applying a non-linear kernel to the output of convolutions using random patches can result in significant improvement in accuracy. With the non-linear kernel, we achieve a test error of 16.4%, which is 9.3% lower than a linear model trained with the same features.

When comparing random features and Nyström after 5 epochs for various values of p , we see that they perform

⁶cs.toronto.edu/~kriz/cifar.html

⁷github.com/akrizhevsky/cuda-convnet2

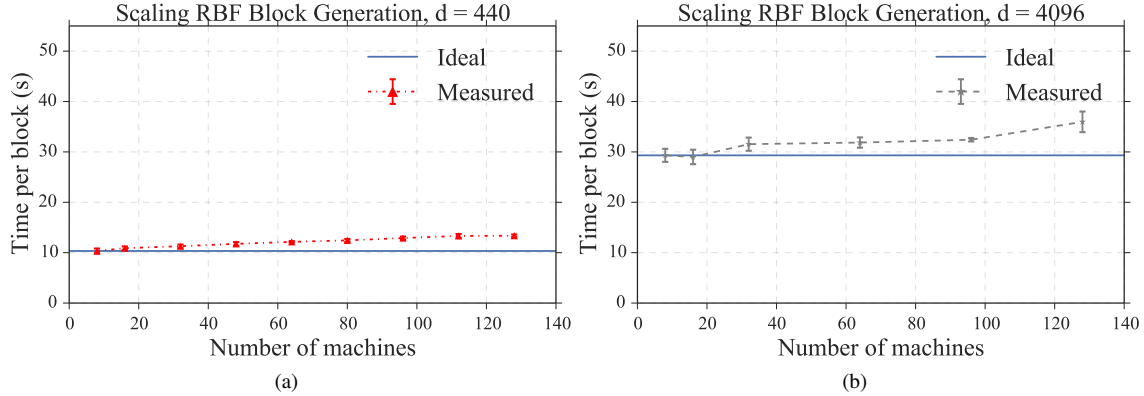


Figure 5: Time taken to compute one block of the RBF kernel as we scale the number of examples and the number of machines used.

similarly for smaller number of features but that random features performs better with larger number of features. We believe that this is due to the Nyström normal equations having a larger condition number for the CIFAR-10 augmented dataset which leads to a worse convergence rate. We verify this in Figures 4(a) and 4(b) by running by Nyström and random feature solvers for 50 epochs. In Figure 4(a), we fix the number of random features to $p \in \{60, 000, 200, 000\}$, and we see that Nyström takes more epochs to converge but reaches a better test error. In Figure 4(b), we perform the same sweep as in Figure 2(c) except we stop at 50 epochs instead of 5. Indeed, when we do this, the difference between Nyström and random features matches the trends in Figures 2(a) and 2(b).

5.4 Performance

We next study the runtime performance characteristics of each method. Figure 3 shows a timing breakdown for running *one block* of block coordinate descent on the three datasets. From the figure, we see that the choice of the kernel approximation can significantly impact performance since different kernels take different amounts of time to generate. For example, the hash random feature used for the Yelp dataset is much cheaper to compute than the string kernel. However, computing a block of the RBF kernel is similar in cost to computing a block of random cosine features. This results in similar performance characteristics for the Nyström and random feature methods on TIMIT.

We also observe that the full kernel takes the least amount of time to solve one block. This is primarily because the full kernel does not compute a gram matrix $Z_b^T Z_b$ and only extracts a block of the kernel matrix K_{bb} . Thus, when the number of blocks is small, as is the case for CIFAR-10 in Figure 1(c), the full kernel’s performance becomes comparable to the Nyström method.

5.5 Scalability of RBF kernel generation

Figure 3 also demonstrates that computing the gram matrix and generating the kernel block are the two most expensive steps in our algorithm. Computing the gram matrix uses distributed matrix multiplication, which is well studied [VDGW97]. To see how the cost of kernel generation changes as dataset size grows, we perform a weak scaling experiment where we increase the number of examples and the number of machines used while keeping the number of examples per machine constant ($n = 16, 384$). We run this experiment for $d = 440$ and $d = 4096$, which are the number of features in TIMIT and CIFAR-10 respectively. Figure 5 contains results from this experiment. In the weak scaling scenario, ideal scaling implies that the time to generate a block of the kernel matrix remains constant as we increase both the data and the number of machines. However, computing a block of the RBF kernel involves broadcasting a $b \times d$ matrix to all the machines in the cluster. This causes a slight decrease in performance as we go from 8 to 128 machines. As broadcast routines scale as $O(\log M)$, we believe that our kernel block generation methods will continue to scale well for larger datasets.

6 Conclusion

This paper shows that scalable kernel machines are feasible with distributed computation. There are several theoretical and experimental continuations of this work.

On the theoretical side, a limitation of our current analysis of block coordinate descent is that we cannot hope to achieve rates better than gradient descent. We believe it is possible to leverage the direct solve in (5) to improve our rate, since when $b = d$ the algorithm reduces to Newton’s method. We are also interested in seeing if acceleration techniques can be applied to substantially reduce the number of iterations needed.

On the experimental side, we would like to extend our algorithm to handle other losses than the square loss; ADMM might be one approach for this. More broadly, since solving a least squares program is a core primitive for many optimization algorithms, we are interested to see if our techniques can be applied in other domains.

Acknowledgements

The authors thank Vikas Sindhwani and the IBM corporation for providing access to the derived TIMIT dataset used in our experiments. BR is generously supported by ONR awards N00014-14-1-0024, N00014-15-1-2620, and N00014-13-1-0129, and NSF awards CCF-1148243 and CCF-1217058. RR is supported by the U.S. Department of Energy under award numbers DE-SC0008700 and AC02-05CH11231. This research is supported in part by NSF CISE Expeditions Award CCF-1139158, LBNL Award 7076018, DARPA XData Award FA8750-12-2-0331, and gifts from Amazon Web Services, Google, SAP, The Thomas and Stacey Siebel Foundation, Adatao, Adobe, Apple, Inc., Blue Goji, Bosch, C3Energy, Cisco, Cray, Cloudera, EMC2, Ericsson, Facebook, Guavus, HP, Huawei, Informatica, Intel, Microsoft, NetApp, Pivotal, Samsung, Schlumberger, Splunk, Virdata and VMware.

References

- [AD11] Alekh Agarwal and John C. Duchi. Distributed delayed stochastic optimization. In *NIPS*, 2011.
- [AKK⁺13] Alekh Agarwal, Sham M. Kakade, Nikos Karampatziakis, Le Song, and Gregory Valiant. Least squares revisited: Scalable approaches for multi-class prediction. In *ICML*, 2013.
- [Bac13] Francis Bach. Sharp analysis of low-rank kernel matrix approximations. In *COLT*, 2013.
- [BJ05] Francis Bach and Michael I. Jordan. Predictive low-rank decomposition for kernel methods. In *ICML*, 2005.
- [BPC⁺11] Stephen Boyd, Neal Parikh, Eric Chu, Borja Peleato, and Jonathan Eckstein. Distributed optimization and statistical learning via the alternating direction method of multipliers. *Foundations and Trends in Machine Learning*, 3(1):1–122, 2011.
- [Bra06] Mikio L. Braun. Accurate error bounds for the eigenvalues of the kernel matrix. *Journal of Machine Learning Research*, 2006.
- [BT89] Dimitri P. Bertsekas and John N. Tsitsiklis. *Parallel and distributed computation: numerical methods*. Prentice-Hall, Inc., 1989.
- [CN12] Adam Coates and Andrew Y. Ng. Learning feature representations with k-means. In *Neural Networks: Tricks of the Trade*. Springer, 2012.
- [DFH15] Lee H. Dicker, Dean P. Foster, and Daniel Hsu. Kernel methods and regularization techniques for nonparametric regression: Minimax optimality and adaptation. <http://www.stat.rutgers.edu/home/ldicker/papers/kernels.pdf>, 2015.
- [DM05] Petros Drineas and Michael W. Mahoney. On the nyström method for approximating a gram matrix for improved kernel-based learning. *Journal of Machine Learning Research*, 2005.

- [EM15] Ahmed El Alaoui and Michael W. Mahoney. Fast randomized kernel methods with statistical guarantees. In *NIPS*, 2015.
- [FCL05] Rong-En Fan, Pai-Hsuen Chen, and Chih-Jen Lin. Working set selection using second order information for training support vector machines. *Journal of Machine Learning Research*, 2005.
- [GM13] Alex Gittens and Michael W. Mahoney. Revisiting the nyström method for improved large-scale machine learning. In *ICML*, 2013.
- [HAS⁺14] Po-Sen Huang, Haim Avron, Tara N Sainath, Vikas Sindhwani, and Bhuvana Ramabhadran. Kernel methods match deep neural networks on timit. In *ICASSP*, 2014.
- [HCL⁺08] Cho-Jui Hsieh, Kai-Wei Chang, Chih-Jen Lin, S. Sathiyarajan, and S. Sundararajan. A dual coordinate descent method for large-scale linear svm. In *ICML*, 2008.
- [HNR15] Ahmed Hefny, Deanna Needell, and Aaditya Ramdas. Rows vs. columns: Randomized kaczmarz or gauss-seidel for ridge regression. *arXiv*, arXiv:1507.05844, 2015.
- [Joa99] Thorsten Joachims. Making large-scale SVM learning practical. In *Advances in Kernel Methods - Support Vector Learning*. MIT Press, 1999.
- [JST⁺14] Martin Jaggi, Virginia Smith, Martin Takáč, Jonathan Terhorst, Sanjay Krishnan, Thomas Hofmann, and Michael I. Jordan. Communication-efficient distributed dual coordinate ascent. In *NIPS*, 2014.
- [LWR⁺15] Ji Liu, Stephen J Wright, Christopher Ré, Victor Bittorf, and Srikrishna Sridhar. An asynchronous parallel stochastic coordinate descent algorithm. *Journal of Machine Learning Research*, 16(1):285–322, 2015.
- [MSJ⁺15] Chenxin Ma, Virginia Smith, Martin Jaggi, Michael I. Jordan, Peter Richtárik, and Martin Takáč. Adding vs. averaging in distributed primal-dual optimization. In *ICML*, 2015.
- [NRRW11] Feng Niu, Benjamin Recht, Christopher Ré, and Stephen J. Wright. Hogwild!: A lock-free approach to parallelizing stochastic gradient descent. In *NIPS*, 2011.
- [Pla98] John Platt. Sequential minimal optimization: A fast algorithm for training support vector machines. Technical Report MSR-TR-98-14, Microsoft Research, 1998.
- [RCR15] Alessandro Rudi, Raffaello Camoriano, and Lorenzo Rosasco. Less is more: Nyström computational regularization. In *NIPS*, 2015.
- [Rif02] Ryan Rifkin. *Everything old is new again: a fresh look at historical approaches in machine learning*. PhD thesis, MIT, 2002.
- [RK04] Ryan Rifkin and Aldebaro Klautau. In defense of one-vs-all classification. *Journal of Machine Learning Research*, 2004.
- [RR07] Ali Rahimi and Benjamin Recht. Random features for large-scale kernel machines. In *NIPS*, 2007.
- [RT13] Peter Richtárik and Martin Takáč. Distributed coordinate descent method for learning with big data. *arXiv*, arXiv:1310.2059, 2013.
- [SRR07] Sören Sonnenburg, Gunnar Rätsch, and Konrad Rieck. Large scale learning with string kernels. In *Large Scale Kernel Machines*. MIT Press, 2007.
- [SS01] Bernhard Schölkopf and Alexander J. Smola. *Learning with kernels*. MIT Press, 2001.
- [SSZ13] Shai Shalev-Shwartz and Tong Zhang. Stochastic dual coordinate ascent methods for regularized loss minimization. *Journal of Machine Learning Research*, 2013.

- [Tro11] Joel A. Tropp. Improved analysis of the subsampled randomized hadamard transform. *Advances in Adaptive Data Analysis*, 3(1–2), 2011.
- [Tro15] Joel A. Tropp. An introduction to matrix concentration inequalities. *Foundations and Trends in Machine Learning*, 2015.
- [VDGW97] Robert A. Van De Geijn and Jerrell Watts. Summa: Scalable universal matrix multiplication algorithm. *Concurrency-Practice and Experience*, 9(4):255–274, 1997.
- [WDL⁺09] Kilian Weinberger, Anirban Dasgupta, John Langford, Alex Smola, and Josh Attenberg. Feature hashing for large scale multitask learning. In *ICML*, 2009.
- [Wri15] Stephen J. Wright. Coordinate descent algorithms. *Mathematical Programming*, 151(1), 2015.
- [WS01] Christopher Williams and Matthias Seeger. Using the nyström method to speed up kernel machines. In *NIPS*, 2001.
- [Yan13] Tianbao Yang. Trading computation for communication: Distributed stochastic dual coordinate ascent. In *NIPS*, 2013.
- [YHCL10] Hsiang-Fu Yu, Cho-Jui Hsieh, Kai-Wei Chang, and Chih-Jen Lin. Large linear classification when data cannot fit in memory. In *KDD*, 2010.
- [YLM⁺12] Tianbao Yang, Yu-Feng Li, Mehrdad Mahdavi, Rong Jin, and Zhi-Hua Zhou. Nyström method vs random fourier features: A theoretical and empirical comparison. In *NIPS*, 2012.
- [ZCD⁺12] Matei Zaharia, Mosharaf Chowdhury, Tathagata Das, Ankur Dave, Justin Ma, Murphy McCauley, Michael J. Franklin, Scott Shenker, and Ion Stoica. Resilient distributed datasets: A fault-tolerant abstraction for in-memory cluster computing. In *NSDI*, 2012.
- [ZKR14] Ce Zhang, Arun Kumar, and Christopher Ré. Materialization optimizations for feature selection workloads. In *SIGMOD*, 2014.
- [ZWSL11] Martin A. Zinkevich, Markus Weimer, Alex Smola, and Lihong Li. Parallelized stochastic gradient descent. In *NIPS*, 2011.

A Proof of Theorem 4.1

Recall that $f : \mathbb{R}^d \rightarrow \mathbb{R}^d$ is a strongly convex and smooth quadratic function with Hessian $\nabla^2 f \in \mathbb{R}^{d \times d}$. Recall we also assume that $mI_d \preceq \nabla^2 f \preceq LI_d$.

Notation. Let $[d] := \{1, \dots, d\}$, $b \in [d]$ be a block size, and let $I \in \Omega_b := \{x \in 2^{[d]} : |x| = b\}$ denote an index set. Recall that $P_I : \mathbb{R}^d \rightarrow \mathbb{R}^d$ is the projection operator that zeros out all the coordinates of the input vector not in I , i.e. $(P_I w)_i = w_i \mathbf{1}_{i \in I}$, where w_i denotes the i -th coordinate of a vector w . It is easy to see that P_I in matrix form is $P_I = \text{diag}(\mathbf{1}_{1 \in I}, \dots, \mathbf{1}_{d \in I}) \in \mathbb{R}^{d \times d}$.

Block Lipschitz constants. We now define a restricted notion of Lipschitz continuity which works on blocks. For an index set I , define

$$L_I := \sup_{w \in \mathbb{R}^d : \|w\|=1} \langle P_I w, \nabla^2 f P_I w \rangle = \lambda_{\max}(P_I \nabla^2 f P_I), \quad L_{\max, b} := \max_{I \in \Omega_b} L_I.$$

Update rule. Recall that block coordinate descent works by fixing some $w^0 \in \mathbb{R}^d$ and iterating the mapping

$$w^{k+1} \leftarrow \underset{w \in \mathbb{R}^d}{\operatorname{argmin}} f(P_{I_k} w + P_{I_k^c} w^k), \quad (9)$$

where $I_0, I_1, \dots \in \Omega_b$ are chosen by some (random) strategy. A common choice is to choose I_k uniformly at random from Ω_b , and to make this choice independent of the history up to time k . This is the sampling strategy we will study. We now have enough notation to state and prove our basic inequality for coordinate descent. This is not new, but we record it for completeness, and because it is simple.

Proposition A.1. *For every $k \geq 0$, we have that the $k + 1$ -th iterate satisfies the inequality*

$$f(w^{k+1}) \leq f(w^k) - \frac{1}{2L_{I_k}} \|P_{I_k} \nabla f(w^k)\|^2. \quad (10)$$

Proof. Put $z^k := w^k - \alpha_k P_{I_k} \nabla f(w^k)$. The update equation in (9) gives us, trivially, for any $\alpha_k \in \mathbb{R}$,

$$f(w^{k+1}) \leq f(z^k).$$

Now, by Taylor's theorem, for some $t \in (0, 1)$, setting $\alpha_k := 1/L_{I_k}$,

$$\begin{aligned} f(z^k) &= f(w^k) - \alpha_k \langle P_{I_k} \nabla f(w^k), \nabla f(w^k) \rangle + \frac{\alpha_k^2}{2} \langle P_{I_k} \nabla f(w^k), \nabla^2 f(tw^k + (1-t)(z^k - w^k)) P_{I_k} \nabla f(w^k) \rangle \\ &\stackrel{(a)}{\leq} f(w^k) - \alpha_k \|P_{I_k} \nabla f(w^k)\|^2 + \frac{L_{I_k} \alpha_k^2}{2} \|P_{I_k} \nabla f(w^k)\|^2 \\ &= f(w^k) - \frac{1}{2L_{I_k}} \|P_{I_k} \nabla f(w^k)\|^2. \end{aligned}$$

where (a) uses the fact that Euclidean projection is idempotent and also the definition of L_{I_k} . \square

We now prove a structural result. The main idea is as follows. Suppose we have some subset $\mathcal{G} \subset \Omega_b$ where $\max_{I \in \mathcal{G}} L_I$ is much smaller compared to $L_{\max, b}$. If this subset is a significant portion of Ω_b , then we expect to be able to improve the basic rate. The following result lays the groundwork for us to be able to make this kind of claim.

Lemma A.2. *Let $\mathcal{G} \subset \Omega_b$ be such that $\frac{|\mathcal{G}^c|}{|\Omega_b|} = \alpha \frac{b}{d}$ for $\alpha \in [0, 1]$. Let each I_k be independent and drawn uniformly from Ω_b . Then, after τ iterations, the iterate w^τ satisfies*

$$\mathbb{E}f(w^\tau) - f_* \leq \left(1 - \frac{b}{d} \left((1 - \alpha) \frac{m}{\max_{I \in \mathcal{G}} L_I} + \alpha \frac{m}{L_{\max, t}} \right) \right)^\tau (f(w^0) - f_*).$$

Proof. The basic proof structure is based on Theorem 1 of [Wri15]. The idea here is to compute the conditional expectation of $\frac{1}{L_{I_k}} \|P_{I_k} \nabla f(w^k)\|^2$ w.r.t. w^k , taking advantage of the structure provided by \mathcal{G} . Put $t := \max_{I \in \mathcal{G}} L_I$. Then,

$$\begin{aligned} \mathbb{E}\left(\frac{1}{L_{I_k}} \|P_{I_k} \nabla f(w^k)\|^2 \mid w^k\right) &= \mathbb{E}\left(\frac{1}{L_{I_k}} \|P_{I_k} \nabla f(w^k)\|^2 \mathbf{1}_{I_k \in \mathcal{G}} \mid w^k\right) + \mathbb{E}\left(\frac{1}{L_{I_k}} \|P_{I_k} \nabla f(w^k)\|^2 \mathbf{1}_{I_k \notin \mathcal{G}} \mid w^k\right) \\ &\geq \frac{1}{t} \mathbb{E}(\|P_{I_k} \nabla f(w^k)\|^2 \mathbf{1}_{I_k \in \mathcal{G}} \mid w^k) + \frac{1}{L_{\max, b}} \mathbb{E}(\|P_{I_k} \nabla f(w^k)\|^2 \mathbf{1}_{I_k \notin \mathcal{G}} \mid w^k) \\ &= \nabla f(w^k)^\top \mathbb{E}\left(\frac{1}{t} P_{I_k} \mathbf{1}_{I_k \in \mathcal{G}} + \frac{1}{L_{\max, b}} P_{I_k} \mathbf{1}_{I_k \notin \mathcal{G}}\right) \nabla f(w^k) \\ &\stackrel{(a)}{=} \nabla f(w^k)^\top \mathbb{E} Q_{I_k} \nabla f(w^k) \\ &\geq \lambda_{\min}(\mathbb{E} Q_{I_k}) \|\nabla f(w^k)\|^2, \end{aligned} \quad (11)$$

where in (a) we define Q_I to be diagonal PSD matrix $Q_I := \frac{1}{t}P_I\mathbf{1}_{I \in \mathcal{G}} + \frac{1}{L_{\max,b}}P_I\mathbf{1}_{I \notin \mathcal{G}}$. Let us look at $(\mathbb{E}Q_{I_k})_{\ell\ell}$. It is not hard to see that

$$|\Omega_b|(\mathbb{E}Q_{I_k})_{\ell\ell} = \frac{1}{t}|\{I \in \mathcal{G} : \ell \in I\}| + \frac{1}{L_{\max,b}}|\{I \in \mathcal{G}^c : \ell \in I\}|.$$

We know that $|\{I \in \mathcal{G} : \ell \in I\}| + |\{I \in \mathcal{G}^c : \ell \in I\}| = |\Omega_b|\frac{b}{d}$. Since $t \leq L_{\max,b}$, the quantity above is lower bounded when we make $|\{I \in \mathcal{G}^c : \ell \in I\}|$ as large as possible. Therefore, since we assume that $|\mathcal{G}^c| \leq |\Omega_b|\frac{b}{d}$,

$$\frac{1}{t}|\{I \in \mathcal{G} : \ell \in I\}| + \frac{1}{L_{\max,b}}|\{I \in \mathcal{G}^c : \ell \in I\}| \geq \frac{1}{t} \left(|\Omega_b|\frac{b}{d} - |\mathcal{G}^c| \right) + \frac{1}{L_{\max,b}}|\mathcal{G}^c|,$$

from which we conclude

$$\lambda_{\min}(\mathbb{E}Q_{I_k}) \geq \frac{1}{t} \left(\frac{b}{d} - \frac{|\mathcal{G}^c|}{|\Omega_b|} \right) + \frac{1}{L_{\max,b}} \frac{|\mathcal{G}^c|}{|\Omega_b|} = \frac{b}{d} \left((1 - \alpha)\frac{1}{t} + \alpha \frac{1}{L_{\max,t}} \right). \quad (12)$$

Combining (11) and (12) with Proposition A.1 followed by iterating expectations, we conclude that

$$\mathbb{E}f(w^{k+1}) \leq \mathbb{E}f(w^k) - \frac{1}{2} \frac{b}{d} \left((1 - \alpha)\frac{1}{t} + \alpha \frac{1}{L_{\max,t}} \right) \mathbb{E}\|\nabla f(w^k)\|^2.$$

The rest of the proof proceeds identically to Theorem 1 of [Wri15], using m -strong convexity to control $\|\nabla f(w^k)\|^2$ from below. \square

The remainder of the proof involves showing the existence of a set $\mathcal{J} \subset \Omega_b$ that satisfies the hypothesis of Lemma A.2. To show this, we need some basic tools from random matrix theory. The following matrix Chernoff inequality is Theorem 2.2 from [Tro11].

Theorem A.3. *Let \mathcal{X} be a finite set of PSD matrices of dimension k , and suppose $\max_{X \in \mathcal{X}} \lambda_{\max}(X) \leq B$. Sample $\{X_1, \dots, X_\ell\}$ uniformly at random from \mathcal{X} without replacement. Put $\mu_{\max} := \ell \cdot \lambda_{\max}(\mathbb{E}X_1)$. Then, for any $\delta \geq 0$,*

$$\mathbb{P} \left\{ \lambda_{\max} \left(\sum_{j=1}^{\ell} X_j \right) \geq (1 + \delta)\mu_{\max} \right\} \leq k \cdot \left[\frac{e^\delta}{(1 + \delta)^{1+\delta}} \right]^{\mu_{\max}/B}.$$

The inequality of Theorem A.3 can be weakened to a more useful form, which we will use directly (see e.g. Section 5.1 of [Tro15]). The following bound holds for all $t \geq e$,

$$\mathbb{P} \left\{ \lambda_{\max} \left(\sum_{j=1}^{\ell} X_j \right) \geq t\mu_{\max} \right\} \leq k \cdot (e/t)^{t\mu_{\max}/B}. \quad (13)$$

We now prove, for arbitrary fixed matrices, a result which controls the behavior of the top singular value of submatrices of our original matrix. Let $A \in \mathbb{R}^{n \times p}$ be fixed. Define for any $t > 0$,

$$\mathcal{J}_t(A) := \left\{ I \in \Omega_b : \lambda_{\max}(P_I^\top A^\top A P_I) < \frac{tb}{p} \lambda_{\max}(A^\top A) \right\}.$$

We now establish a result controlling the size of $\mathcal{J}_t(A)$ from below. We do this via a probabilistic argument, taking advantage of the matrix Chernoff inequality.

Lemma A.4. *Fix an $A \in \mathbb{R}^{n \times p}$ and $b \in \{1, \dots, p\}$ and $\delta \in (0, 1)$. Suppose that I is drawn uniformly at random from Ω_b . We have that*

$$\mathbb{P} \left\{ \lambda_{\max}(P_I A^\top A P_I) \geq e^2 \frac{b}{p} \lambda_{\max}(A^\top A) + \|\text{diag}(A^\top A)\|_\infty \log \left(\frac{n}{\delta} \right) \right\} \leq \delta.$$

Proof. This argument closely follows Section 5.2.1 of [Tro15]. First, we observe that we can write AP_I as $AP_I = \sum_{i=1}^p \mathbf{1}_{\{i \in I\}} A_{:i} e_i^\top$, where $A_{:i} \in \mathbb{R}^n$ denotes the i -th column of A . Also, since $\lambda_{\max}(P_I^\top A^\top AP_I) = \lambda_{\max}(AP_I P_I^\top A^\top)$, we focus our efforts on the latter. Now,

$$AP_I P_I^\top A^\top = \left(\sum_{i=1}^p \mathbf{1}_{\{i \in I\}} A_{:i} e_i^\top \right) \left(\sum_{i=1}^p \mathbf{1}_{\{i \in I\}} A_{:i} e_i^\top \right)^\top = \sum_{i=1}^p \mathbf{1}_{\{i \in I\}} A_{:i} A_{:i}^\top.$$

Let $\mathcal{X} := \{A_{:i} A_{:i}^\top : i \in \{1, \dots, p\}\}$. The calculation above means we can equivalently view the random variable $AP_I P_I^\top A^\top$ as the sum $\sum_{i=1}^b X_i$ where X_1, \dots, X_b are sampled from \mathcal{X} without replacement. Put $\mu_{\max} := b \cdot \lambda_{\max}(\mathbb{E} X_1) = \frac{b}{p} \lambda_{\max}(AA^\top) = \frac{b}{p} \lambda_{\max}(A^\top A)$. Observe that $\max_{1 \leq i \leq p} \lambda_{\max}(A_{:i} A_{:i}^\top) = \max_{1 \leq i \leq p} \|A_{:i}\|^2 := B$. This puts us in a position to apply Theorem A.3, using the form given by (13), from which we conclude for all $t \geq e$,

$$\mathbb{P} \left\{ \lambda_{\max}(P_I^\top A^\top AP_I) \geq \frac{tb}{p} \lambda_{\max}(A^\top A) \right\} \leq n(e/t)^{\frac{tb}{Bp}} \cdot \lambda_{\max}(A^\top A), \quad (14)$$

To conclude, set

$$t = \frac{p}{b} \frac{B}{\lambda_{\max}(A^\top A)} \log \frac{n}{\delta} + e^2, \quad (15)$$

and plug into (14). The result follows by noting that $\max_{1 \leq i \leq p} \|A_{:i}\|^2 = \max_{1 \leq i \leq p} e_i^\top A^\top A e_i = \max_{1 \leq i \leq p} (A^\top A)_{ii}$. \square

We are now in a position to prove Theorem 4.1.

Proof. (Of Theorem 4.1). Let $\nabla^2 f = Q^\top Q$ be a factorization of $\nabla^2 f$ which exists since $\nabla^2 f$ is PSD. Note that we must have $Q \in \mathbb{R}^{d \times d}$ because $\nabla^2 f$ is full rank. Recall that $\lambda_{\max}(Q^\top Q) \leq L$. First, we note that

$$\mathbb{P} \left\{ \lambda_{\max}(P_I^\top A^\top AP_I) \geq \frac{tb}{p} \lambda_{\max}(A^\top A) \right\} = \mathbb{P}(I \in \mathcal{J}_t^c(A)) = \mathbb{E} \mathbf{1}_{\{I \in \mathcal{J}_t^c(A)\}} = \frac{|\mathcal{J}_t^c(A)|}{|\Omega_b|}.$$

Setting t as in (15) and invoking Lemma A.4, we have that every $I \in \mathcal{J}_t(Q)$ satisfies

$$\lambda_{\max}(P_I Q^\top Q P_I) < \|\text{diag}(\nabla^2 f)\|_\infty \log(2d^2/b) + e^2 \frac{b}{d} L.$$

The result follows immediately by an application of Lemma A.2 \square

B Proofs for Section 4.2

B.1 Derivation of rates in Table 2

Full kernel. As noted in Section 3, we actually run Gauss-Seidel on $(K + n\lambda I_n)\alpha = Y$, which can be seen as coordinate descent on the program

$$\min_{\alpha \in \mathbb{R}^{n \times k}} \frac{1}{2} \langle \alpha, K\alpha \rangle + \frac{n\lambda}{2} \|\alpha\|_F^2 - \langle Y, \alpha \rangle.$$

Note that the objective is a strongly convex function with Hessian given as $D^2 f(\alpha)[H, H] = \langle H, (K + n\lambda I_n)H \rangle$. Theorem 4.1 tells us that setting $b \gtrsim n \log n \frac{\|\text{diag}(K + n\lambda I_n)\|_\infty}{\|K + n\lambda I_n\|}$, $\tilde{O}(1/\lambda)$ iterations are sufficient. Plugging values in, we get for $b \gtrsim \log^2 n$ under (a) and $b \gtrsim n^{1/(2\beta+1)} \log n$ under (b), the number of iterations is bounded under (a) by $\tilde{O}(n)$ and under (b) by $\tilde{O}(n^{\frac{2\beta}{2\beta+1}})$.

Nyström approximation. We derive a rate for coordinate descent on (3). We use the regularized variant, which ensures that (3) is strongly convex. Let $p \leq n$ denote the number of Nyström features, let I denote the index set of features, and let $S \in \mathbb{R}^{n \times p}$ be the column selector matrix such that $K_I = KS$. The Hessian of (3) is given by

$$nD^2 f[H, H] = \langle H, (S^\top K(K + n\lambda I_n)S + n\lambda\gamma I_p)H \rangle.$$

Theorem 4.1 tells us that we want to set $b \gtrsim p \log p \frac{\|\text{diag}(S^\top K(K + n\lambda I_n)S + n\lambda\gamma I_p)\|_\infty}{\|S^\top K(K + n\lambda I_n)S + n\lambda\gamma I_p\|}$. Applying a matrix Chernoff argument (Lemma A.4) to control $\|S^\top K(K + n\lambda I_n)S\|$ from above, we have w.h.p. that the number of iterations is $\tilde{O}(p/\lambda\gamma)$. Under (a) this is $\tilde{O}(np/\gamma)$ and under (b) this is $\tilde{O}(pn^{\frac{2\beta}{2\beta+1}}/\gamma)$.

To control b , we apply a matrix Bernstein argument (Lemma B.2) to control $\|S^\top K(K + n\lambda I_n)S\|$ from below w.h.p. This argument shows that when $\lambda \leq O(1)$ and $p \gtrsim \log n$, $\|S^\top K(K + n\lambda I_n)S\| \gtrsim np$, from which we conclude that $b \gtrsim (1 + \gamma) \log n$.

Random features approximation. We now derive a rate for coordinate descent on (4). The Hessian of (4) is given by $nD^2 f(\alpha)[H, H] = \langle H, (Z^\top Z + n\lambda I_p)H \rangle$. Thus by Theorem 4.1, setting $b \gtrsim p \log p \frac{\|\text{diag}(Z^\top Z + n\lambda I_p)\|_\infty}{\|Z^\top Z + n\lambda I_p\|}$ and applying a matrix Bernstein argument to control $\|Z^\top Z + n\lambda I_p\|$ from both directions (Lemma B.4), then as long as $p \gtrsim \log n$, we have w.h.p. that this is at most $\tilde{O}(1/\lambda)$, which is the same rate as the full kernel. Furthermore, the block size is $b \gtrsim \log n$.

B.2 Supporting lemmas for Section B.1

For a fixed symmetric Q and random I , we want to control $\lambda_{\max}(P_I Q P_I)$ from below. The matrix Chernoff arguments do not allow us to do this, so we rely on matrix Bernstein. The following result is Theorem 2 from [EM15].

Theorem B.1. Fix a matrix $\Psi \in \mathbb{R}^{n \times m}$, $p \in \{1, \dots, m\}$ and $\beta \in (0, 1]$. Let $\psi_i \in \mathbb{R}^n$ denote the i -th column of Ψ . Choose $i_k, k = 1, \dots, p$ from $\{1, \dots, m\}$ such that $\mathbb{P}(i_k = j) = p_i \geq \beta \|\psi_i\|^2 / \|\Psi\|_F^2$. Put $\tilde{S} \in \mathbb{R}^{n \times p}$ such that $\tilde{S}_{ij} = 1/\sqrt{p \cdot p_{ij}}$ if $i = i_j$ and 0 otherwise. Then for all $t \geq 0$,

$$\mathbb{P} \left\{ \lambda_{\max}(\Psi\Psi^\top - \Psi\tilde{S}\tilde{S}^\top\Psi^\top) \geq t \right\} \leq n \exp \left(\frac{-pt^2/2}{\lambda_{\max}(\Psi\Psi^\top)(\|\Psi\|_F^2/\beta + t/3)} \right).$$

This paves the way for the following lemma.

Lemma B.2. Fix a matrix $\Psi \in \mathbb{R}^{n \times m}$, $p \in \{1, \dots, m\}$. Let $\psi_i \in \mathbb{R}^n$ denote the i -th column of Ψ . Put $B := \max_{1 \leq i \leq m} \|\psi_i\|^2$. Choose $I := (i_1, \dots, i_p)$ uniformly at random without replacement from $\{1, \dots, m\}$. Let $S \in \mathbb{R}^{n \times p}$ be the column selector matrix associated with I . Then, with probability at least $1 - \delta$ over the randomness of I ,

$$\lambda_{\max}(\Psi S S^\top \Psi^\top) \geq \frac{p}{m} \lambda_{\max}(\Psi\Psi^\top) - \frac{4}{3} \frac{\lambda_{\max}(\Psi\Psi^\top)}{m} \log \left(\frac{n}{\delta} \right) - \sqrt{\frac{8p}{m} \lambda_{\max}(\Psi\Psi^\top) B \log \left(\frac{n}{\delta} \right)}.$$

Proof. Put $p_i = 1/m$ for $i = 1, \dots, m$ and $\beta = \frac{\|\Psi\|_F^2}{mB}$. By definition, $\beta \leq 1$. In this case, $\tilde{S} = \sqrt{\frac{m}{p}} S$. Plugging these constants into Theorem B.1, we get that

$$\mathbb{P} \left\{ \lambda_{\max} \left(\frac{p}{m} \Psi\Psi^\top - \Psi S S^\top \Psi^\top \right) \geq \frac{p}{m} t \right\} \leq n \exp \left(\frac{-pt^2/2}{\lambda_{\max}(\Psi\Psi^\top)(mB + t/3)} \right).$$

Setting the RHS equal to δ , we get that t is the roots of the quadratic equation

$$t^2 - \frac{2}{3} \frac{\lambda_{\max}(\Psi\Psi^\top)}{p} \log \left(\frac{n}{\delta} \right) \cdot t - 2 \lambda_{\max}(\Psi\Psi^\top) \frac{mB}{p} \log \left(\frac{n}{\delta} \right) = 0.$$

Since solutions to $t^2 - at - b = 0$ satisfy $t \leq 2(a + \sqrt{b})$ when $a, b \geq 0$, from this we conclude

$$t \leq \frac{4}{3} \frac{\lambda_{\max}(\Psi\Psi^\top)}{p} \log\left(\frac{n}{\delta}\right) + \sqrt{8\lambda_{\max}(\Psi\Psi^\top) \frac{mB}{p} \log\left(\frac{n}{\delta}\right)}.$$

Hence,

$$\mathbb{P} \left\{ \lambda_{\max}\left(\frac{p}{m} \Psi\Psi^\top - \Psi S S^\top \Psi^\top\right) \geq \frac{4}{3} \frac{\lambda_{\max}(\Psi\Psi^\top)}{m} \log\left(\frac{n}{\delta}\right) + \sqrt{\frac{8p}{m} \lambda_{\max}(\Psi\Psi^\top) B \log\left(\frac{n}{\delta}\right)} \right\} \leq \delta. \quad (16)$$

By the convexity of $\lambda_{\max}(\cdot)$,

$$\frac{p}{m} \lambda_{\max}(\Psi\Psi^\top) = \lambda_{\max}\left(\Psi S S^\top \Psi^\top + \frac{p}{m} \Psi\Psi^\top - \Psi S S^\top \Psi^\top\right) \leq \lambda_{\max}(\Psi S S^\top \Psi^\top) + \lambda_{\max}\left(\frac{p}{m} \Psi\Psi^\top - \Psi S S^\top \Psi^\top\right). \quad (17)$$

Combining (16) and (17) yields the result. \square

We now study random features. To do this, we need the following general variant of matrix Bernstein. The following is Corollary 6.2.1 of [Tro15].

Theorem B.3. *Let $B \in \mathbb{R}^{d_1 \times d_2}$ be a fixed real matrix. Let $R \in \mathbb{R}^{d_1 \times d_2}$ be a random matrix such that $\mathbb{E}R = K$ and $\|R\| \leq L$ a.s. Put*

$$G := \frac{1}{n} \sum_{k=1}^n R_k, \quad m_2(R) := \max\{\|\mathbb{E}R R^\top\|, \|\mathbb{E}R^\top R\|\},$$

where each R_k is an independent copy of R . Then for all $t \geq 0$,

$$\mathbb{P}\{\|G - K\| \geq t\} \leq (d_1 + d_2) \exp\left(\frac{-nt^2/2}{m_2(R) + 2Lt/3}\right).$$

This variant allows us to easily establish the following lemma.

Lemma B.4. *Fix an $\alpha \in (0, 1)$. Let $ZZ^\top \in \mathbb{R}^{n \times n}$ be from the random features construction. Put $B := \sup_{x \in \mathcal{X}} |\varphi(x, \omega)|$, and suppose $B < \infty$. Then with probability at least $1 - \delta$, we have that as long as $p \geq \frac{2}{\alpha} \left(\frac{1}{\alpha} + \frac{2}{3}\right) \frac{nB^2}{\|K\|} \log\left(\frac{2n}{\delta}\right)$,*

$$(1 - \alpha)\|K\| \leq \|ZZ^\top\| \leq (1 + \alpha)\|K\|.$$

Proof. We set up parameters so we can invoke Theorem B.3. This follows Section 6.5.5 of [Tro15]. Define $\xi_k = (\varphi(x_1, \omega_k), \dots, \varphi(x_n, \omega_k)) \in \mathbb{R}^n$ and $R_k = \xi_k \xi_k^\top$. This setting means that $\frac{1}{p} \sum_{k=1}^p R_k = ZZ^\top$. We have $\|R_k\| = \|\xi_k \xi_k^\top\| = \|\xi_k\|^2 \leq nB^2$. Furthermore,

$$\mathbb{E}R_k^2 = \mathbb{E}\|\xi_k\|^2 \xi_k \xi_k^\top \leq nB^2 \mathbb{E}\xi_k \xi_k^\top = nB^2 K \implies m_2(R) \leq nB^2 \|K\|.$$

Hence by Theorem B.3,

$$\mathbb{P}\{\|ZZ^\top - K\| \geq t\} \leq 2n \exp\left(\frac{-pt^2/2}{nB^2\|K\| + 2nB^2t/3}\right).$$

Setting $t = \alpha\|K\|$, we require that $p \geq \frac{2}{\alpha} \left(\frac{1}{\alpha} + \frac{2}{3}\right) \frac{nB^2}{\|K\|} \log\left(\frac{2n}{\delta}\right)$ to ensure that $\mathbb{P}\{\|ZZ^\top - K\| \geq \alpha\|K\|\} \leq \delta$. On the complement on this event, we have that $\|ZZ^\top\| \leq \|K\| + \|ZZ^\top - K\| \leq (1 + \alpha)\|K\|$. Similarly, $\|K\| \leq \|ZZ^\top\| + \|K - ZZ^\top\| \leq \|ZZ^\top\| + \alpha\|K\|$. The result now follows. \square